https://doi.org/10.15255/KUI.2022.065
KUI-19/2023
Original scientific paper
Received October 9, 2022
Accepted January 24, 2023

Prediction of Hourly Global Solar Radiation: Comparison of Neural Networks / Bootstrap Aggregating

A. Dahmani,[a,b,*] *Y. Ammi*,[b] *S. Hanini*,[b] *M. Redha Yaiche*,[c] and *H. Zentou*[d]

[a] Department of Mechanical Engineering, Faculty of Science and Technology, GIDD Industrial Engineering and Sustainable Development Laboratory, University of Relizane, Bourmadia, 48 000, Relizane, Algeria
[b] Laboratory of Biomaterials and Transport Phenomena (LBMPT), University of Medea, Urban pole, 26 000, Medea, Algeria
[c] Renewable Energy Development Center (CDER), Postal Box 62, Observatory Road Bouzareah 16 340, Algiers, Algeria
[d] Department of Chemical and Environmental Engineering, University Putra Malaysia, 43 400 Serdang, Malaysia

Abstract

This research work explores the use of single neural networks and bootstrap aggregated neural networks for predicting hourly global solar radiation. A database of 3606 data points were from the Renewable Energies Development Center, radiometric station 'Shems' of Bouzareah. The single neural networks and bootstrap aggregated neural networks were built together. The precision and durability of neural network models generated with an incomplete quantity of training datasets were improved using bootstrap aggregated neural networks. To produce numerous sets of training data points, the training data was re-sampled utilising bootstrap resampling by replacement. A neural network model was built for each of the data points. The individual neural network models were then combined to produce the bootstrap aggregated neural networks. The experimental and predicted values of global solar radiation were compared, and lower root mean squared errors (68.3968 and 62.4856 Wh m^{-2}) were discovered during the testing phases for single neural networks and bootstrap aggregated neural networks, respectively. The results of these models show that the bootstrap aggregated neural networks model is more accurate and robust than single neural networks.

Keywords

Prediction, hourly global solar radiation, neural networks, bootstrap aggregating

1 Introduction

Solar energy encompasses both heat and light released by the sunshine, which is the result of nuclear processes within the Sun, Earth's nearest star. The quantity of energy developed is significantly more than the world's current energy needs. If it is properly harnessed and used, it might fulfil all future energy needs.[1]

The entire quantity of solar energy absorbed by the Earth's surface is defined as global solar radiation; this quantity is extremely significant in different scientific fields, such as architecture, agriculture, climatology, and solar energy production.[2,3]

Currently, solar radiation and renewable energy have emerged as critical energy technologies that can aid in dealing with climate change challenges. The expansion of the use of renewable energy sources results in a decrease in CO_2 emissions, reduction in local air pollution, the development of high-value professions, and a reduction in a country's reliance on fossil energy imports. When comparing solar energy to other fossil-based energy sources, it is clear that solar energy, a significant source of energy, is not harmful to the environment and has no effect on global warming.[4,5]

The solar radiation data is extremely significant for manufacturers, designers of solar energy systems, architects, and agriculturists. However, solar radiation measurements have only been taken at a few sites around the world due to various reasons, among them being installation costs, maintenance, and calibration.[6] As a result of the significance of the global solar radiation data, several approaches are being utilised to estimate solar radiation from various parameters. Several statistical approaches, such as analysis methods and statistical techniques, are feasible options for estimating solar radiation using a range of meteorological factors.[7–9]

Artificial neural network (ANN) technology has recently received much attention as a computational approach that provides an alternative and integrated modelling method, given its ability to deal with complex and ill-defined problems in many scientific fields. In the meteorological field, many researchers have studied the use of single neural network (SNN) models for predicting global solar radiation, as seen in the literature.[10–24] However, ANN has been reproved for its nature, which lead to difficulties in understanding the linearity or quadratic dependency of the transfer equations. Furthermore, the computational cost, as well as the issue of overfitting, was found.[25]

The available training data and the training procedure have a considerable impact on the quality and resilience

* Corresponding author: Dr Abdennasser Dahmani
Email: dahmani.abdennasser@univ-relizane.dz

of neural network models; otherwise, the neural network would likely overfit noise in the training data and display severe generalisation errors. Developing a variety of neural network models and then combining them is an appealing technique for increasing neural network model resilience. Several academics have applied the combination of different neural network models.[26]

The bootstrap aggregated neural networks (BANN) models were developed by Hansen and Salamon.[27] It is a method for improving a model's generalisation capabilities by training multiple neural networks, which are then combined. This strategy is not only successful but simple to use, as it has been applied in a variety of settings. BANN have been demonstrated to have superior generalisation capabilities over SNNs.[28,29] Several strategies, such as collecting staking neural networks, have been proposed in order to improve the robustness and resilience of neural network models.[30]

Practically all of the established models in the scientific literature contributions are made on the basis of a single artificial neural network arrangement, which is trained to predict the values of solar radiation using different climatic data gathered over the years. By collecting staking neural networks, the adoption of a single structural model can reduce estimation accuracy and slow down the training process, causing the predictive model to diverge and become unstable.[31] The aim of this research work was to improving a BANN model to predict the hourly global solar radiation received on the horizontal plane over one year in the region of Bouzareah (Algeria), using eight meteorological and climatological parameters. According to our knowledge, no studies using bootstrap-based ANN for modelling solar radiation have been described in the literature. Individual neural network (INN) and SNN models were compared with BANN.

1.1 Related studies

A number of studies and research initiatives have attempted to predict solar radiation, the most significant accomplishment in recent years. Different methods have been examined, such as smart persistence (SP), neural network (NN), and random forest (RF), which were compared and evaluated using solar data collected at a high-variability meteorological location; the nRMSE obtained was 22.57 %.[32] An applied ANN model was established to estimate tilted irradiance at different inclinations in Taiwan. The input parameters contained global horizontal irradiance, solar elevation, azimuth cosine, azimuth sine, cosine and sine of pyranometer azimuth, and dip. The model consisted of three hidden layers, each one containing six neurons, total mean nRMSE of 8.02 %.[33] It used meteorological data gathered over a 10-year period from five distinct places throughout India to train the models based on different methods for forecasting monthly average global solar radiation.[34] A backpropagation neural network (BPNN) was used to predict solar irradiance data in different spectral bands from daily time series. Three performance metrics were used to assess the proposed model's ability to forecast solar irradiance, including RMSE, mean systematic error (MBE), and correlation coefficient. The results showed that the model predicted daily solar irradiance more accurately.[35]

Using weather factors, sun angles, and extra-terrestrial irradiance, a neural network model was developed to forecast global irradiance. The findings showed that the suggested model was more efficient in estimating global irradiance than the power persistence forecast model.[36]

Studied was the hourly solar radiation received on the horizontal plane in Ghardaïa city (Algeria) using an SNN model with the quasi-Newton backpropagation (BFGS) as activation function, and useful weights method to find the importance of all input parameters.[15] The best results were obtained with a root mean square error (RMSE) of 4.71 %. These findings proposed that the optimised model was stable and had a strong predictive capacity.

Rezrazi et al. demonstrated how to reach an optimum ANN model for solar radiation prediction. The optimisation process was demonstrated using measured data from Ghardaïa city in 2007. The performance of ANN models was evaluated, and the results were compared with measured data by mean absolute percentage error (MAPE). The MAPE in the ANN optimum model was determined to be 1.17 %. This model also had a 14.06 % root mean square error (RMSE), and a 0.12 % MBE. The collected results showed that the optimisation technique had met practical criteria. It may be generalised to any point on Earth, and utilized in applications other than solar radiation estimation.[37] Detected was the capacity of multilayer perceptron to create very short-time irradiation estimations (5 min) in Bouzareah over 2 years. The entered parameter used declination zenith angle and azimuth. The average nRMSE was found to be 8.81 %, which is excellent accuracy for such a short time step.[3]

In this context, in the present research work, we applied and developed a method of BANN based on SNN for improving robust non-linear models for predicting hourly global solar radiation in Bouzareah.

2 Material and methods

2.1 Studied region and data collection

The database of users in this research work was collected from the radiometric station 'Shems' belonging to the Center for Renewable Energy Development (CDER) of Bouzareah, in Algiers, with latitude 36.8 °N, longitude 3.17 °E, and altitude 345 m. These data were recorded over one year (January 1 – December 31, 2015). A Mediterranean climate prevails at the location, with dry, hot summers, and damp, chilly winters (Fig. 1).

This database (DB) has 3606 points. It was used with the objective of optimising bootstrapped aggregated neural networks (BANN) parameters. In the database, we excluded all values less than 120 W m^{-2} (from 5 to 17 h) based on the world meteorological organisation that defines the sunshine duration when the global solar radiation values are higher than 120 W m^{-2}.[39]

Fig. 1 – Location of the CDER meteorological station in Bouzareah[38]

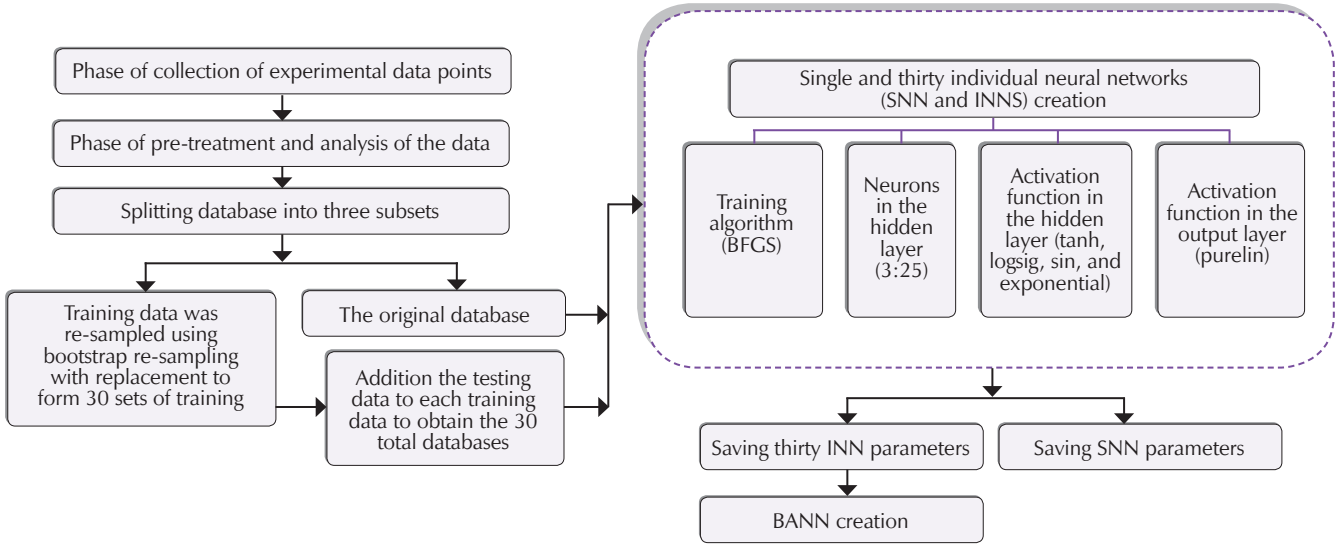

Fig. 2 – Neural network development (SNN, INN, and $BANN_{(Stacking\ of\ 30\ networks)}$)[40]

2.2 Modelling procedure

2.2.1 Single neural networks

ANNs were inspired by the way natural neurons process information. Neurons are individual cells that are combined to create a dense network of around 10–100 billion linked units in the human brain. There are four components of a biological neuron: 1) dendrites represent the principal part of the inputs of neurons that receive information and commands from other neurons; 2) cell body contains the nucleus of the nerve cell; it is the information processing centre; 3) axon is the neuron's output and the bearer of information to the rest of the brain's neurons; 4) synapses are the synaptic weights of formal neurons that link neurons with each other.

The neurons are the most significant element of neural networks and have a highly capable mathematical base and direct values.[40]

SNN includes three layers: input, hidden, and output layers. Compute units make up the layers, which are connected *via* transfer functions. The neurons of each layer are connected with the neurons of the adjacent layer through connections called synaptic weights w_{ij}, affecting the influence of each input on the output of the neuron. Each neuron integrates all the signals from the neurons of the previous layer according to an activation function.[41] Fig. 2 shows a technique for designing and optimising the architecture of INN and SNN.

The statistical investigation of the overall data was done in terms of the minimum "min", the average "mean", the maximum "max", "sum", variance "Var", and the standard deviation "STD" as shown in Table 1.

2.2.2 Bootstrap aggregated neural networks

Developing a variety of ANN models and then combining them is an appealing technique for increasing this model's robustness. Many academic researchers have looked into combining different neural network models[42,26] to construct BANN models, the training data set was re-sampled using bootstrap re-sampling with replacement[43,44] to create 30 training sets.

BANN are depicted in Fig 3. When numerous independent neural network models are developed to model the same relationship, the equation below is used to combine them:

$$y = \frac{\sum_{i=1}^{n} y_i}{n} \tag{1}$$

where y_i represents the output of INN, y represents the output of the BANN, and n is the number of INN models.

Each model was given its own neural network (SNN and BANN). Every ANN contains three layers of neurons: an

Table 1 – Numerical analysis of inputs and output

		Min	Mean	Max	Std	Var	Sum
Inputs	Month	1.000	6.484	12.000	3.167	10.031	23361.000
	Day	1.000	15.715	31.000	8.814	77.691	56619.000
	Time / h	5.000	11.337	17.000	3.020	9.120	40847.000
	Temperature / K	280.260	294.682	308.540	6.220	38.693	1061700.000
	Relative Humidity / %	22.880	58.611	95.000	11.401	129.976	211170.000
	Pressure / mbar	972.590	996.482	1020.200	6.242	38.962	3590300.000
	Wind speed / m s^{-1}	0.080	4.292	16.590	2.227	4.959	15465.000
	Wind direction / °	0.020	172.060	359.780	118.352	14007.000	619930.000
Outputs	Global solar radiation / Wh m^{-2}	120.010	515.576	1030.723	247.880	61444.000	1857600.000

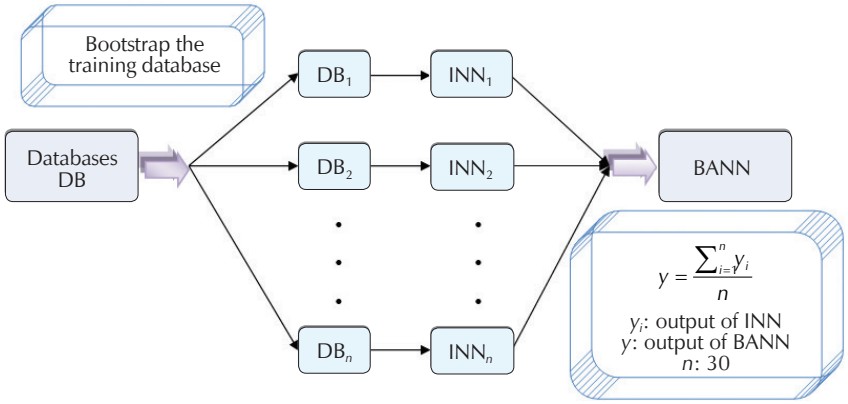

Fig. 3 – Bootstrap aggregated neural networks[40]

input layer with eight neurons, a hidden layer with many neurons regulated during training, and an output layer with one unit that generates the value of global solar radiation prediction. The number of hidden neurons ranged from three to twenty-five in this study. The logistic sigmoid (logsig), the tangent hyperbolic (tanh), the sine function, and the exponential activation function were applied in the hidden layer. The pure-linear (purelin) activation function was utilised in the output layer. All neural networks were trained by the BFGS quasi-Newton (trainbfg).

The average of the INN outputs was used to calculate the BANN output. STATISTICA and MATLAB 2020b tools were used to apply ANN to the prediction of hourly global solar radiation.

3 Results and discussion

3.1 Effect of the division of the database

We partitioned the total database into three sections: Section 1 (2886 points for training (80 %), 360 for validation (10 %), and 360 for testing (10 %)); Section 2 (2524 points for training (70 %), 541 for validation (15 %), and 541 for testing (15 %)), and Section 3 (2164 points for training (60 %), 721 for validation (20 %), and 721 for testing (20 %).

Fig. 4 shows the global solar radiation as a function of temperature for the total database. It is clear that global solar radiation increases with increasing temperature at some points.

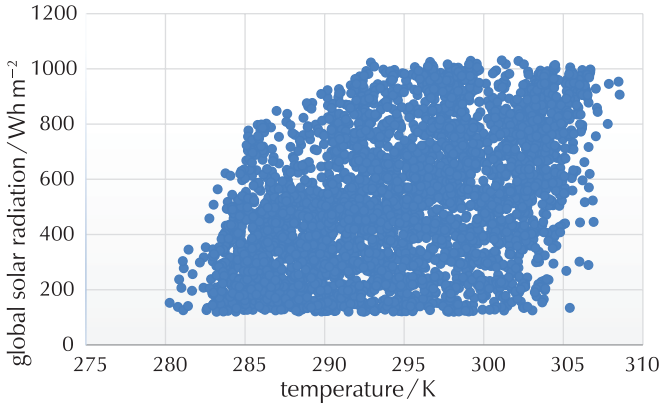

Fig. 4 – Global solar radiation (GSR, Wh m^{-2}) is a function of temperature (K)

Table 2 shows the coefficient of correlation (*R*) and the root mean squared error (RMSE) obtained for predicting hourly global solar radiation under the impact of the division of the database for the SNN model. The results show that Section 1 was the optimal division, as it gave better results than the other divisions for the testing phase. The INN were then developed using Section 1 of the data set.

Table 2 – Influence of the division of the database for SNN

	Database	Percentage /%	RMSE / W m^{-2}	*R*
Section 1	Training phase: 2886 data points	80	67.2010	0.9624
	Validation phase: 360 data points	10	75.3743	0.9540
	Testing phase: 360 data points	10	**68.3968**	0.9618
Section 2	Training phase: 2524 data points	70	65.1957	0.9649
	Validation phase: 541 data points	15	74.5834	0.9551
	Testing phase: 541 data points	15	73.9391	0.9529
Section 3	Training phase: 2164 data points	60	69.3676	0.9604
	Validation phase: 721 data points	20	75.1032	0.9537
	Testing phase: 721 data points	20	76.1473	0.9496

3.2 Performance models

Table 3 shows the architecture of the INN and SNN models. The INN and SNN are not harmonic, as may be seen, and are given diverse structures. Fifteen INNs applied the activation function log sigmoid (logistic), and thirteen tangent hyperbolic (tanh) activation function, the same activation that gives the SNN model its efficiency, dependability, and resilience. The activation function exponential was utilised in the hidden layer of two individual neural networks; however, the function sin was not employed in the hidden layer of neural networks. Thus, we determined the supremacy of the activation functions (tanh and sigmoid) over the functions (sin and exponential), and these findings corroborate the findings of *Kiseľák et al.*[45] and *Ammi et al.*[40]

According to this analytical discussion, two types of neural network models were developed (SNN and $BANN_{(Stacking\ of\ 30\ networks)}$) with the goal of predicting hourly global solar radiation on a horizontal plane. Fig. 5 presents a comparison between the experimental and calculated value of hourly global solar radiation with vectors of agreement near the optimisation of neural network profiles, for SNN ($R = 0.9537$ for the validation phase and $R = 0.9618$ for the test phase), and for $BANN_{(Staking\ of\ 30\ networks)}$ ($R = 0.9566$ for validation data, and 0.9680 for test data). In both the SNN and BANN models, the slope is near 1 during the validation phase, and it is extremely near 1 during the testing phase. The intercept *b* is distant from 0 for the validation and testing phases in the two models (SNN) and (BANN). In general, the correlation coefficients are assumed excellent when ($0.9000 \leq R \leq 1.0000$) for these models (SNN and BANN); this demonstrates the resilience of existing neural network models as well as the ability to predict hourly global solar radiation.

Table 3 – Characteristics of INN models

INN	Neurons number in the hidden layer	Activation function in the hidden layer	INN	Neurons number in the hidden layer	Activation function in the hidden layer
INN_1	22	Tanh	INN_{16}	24	Logsig
INN_2	22	Logsig	INN_{17}	24	Exponential
INN_3	23	Tanh	INN_{18}	25	Tanh
INN_4	21	Logsig	INN_{19}	22	Logsig
INN_5	23	Logsig	INN_{20}	11	Tanh
INN_6	20	Exponential	INN_{21}	17	Logsig
INN_7	21	Tanh	INN_{22}	22	Tanh
INN_8	17	Logsig	INN_{23}	20	Logsig
INN_9	19	Logsig	INN_{24}	10	Tanh
INN_{10}	19	Logsig	INN_{25}	19	Tanh
INN_{11}	14	Logsig	INN_{26}	18	Logsig
INN_{12}	24	Tanh	INN_{27}	23	Tanh
INN_{13}	22	Tanh	INN_{28}	15	Tanh
INN_{14}	21	Logsig	INN_{29}	21	Logsig
INN_{15}	20	Logsig	INN_{30}	24	Tanh

3.3 Analysis and comparison between individual neural networks

Fig. 6 presents the different measured errors to determine the level of quality prediction models: the model predictive error MPE, the root mean squared error RMSE, and the standard error of prediction SEP. It can be observed that these networks are not consistent, with INNs performing differently in different phases. The following are the equations for those errors:

$$\mathrm{MPE}(\%) = \frac{100}{n}\sum_{i=1}^{n}\left|\frac{(y_{i,\mathrm{exp}} - y_{i,\mathrm{cal}})}{y_{i,\mathrm{exp}}}\right| \tag{2}$$

$$\mathrm{RMSE} = \sqrt{\frac{\sum_{i=1}^{n}\left(y_{i,\mathrm{exp}} - y_{i,\mathrm{cal}}\right)^2}{n}} \tag{3}$$

$$\mathrm{SEP}(\%) = \frac{\mathrm{RMSE}}{y_{\mathrm{e}}} \cdot 100 \tag{4}$$

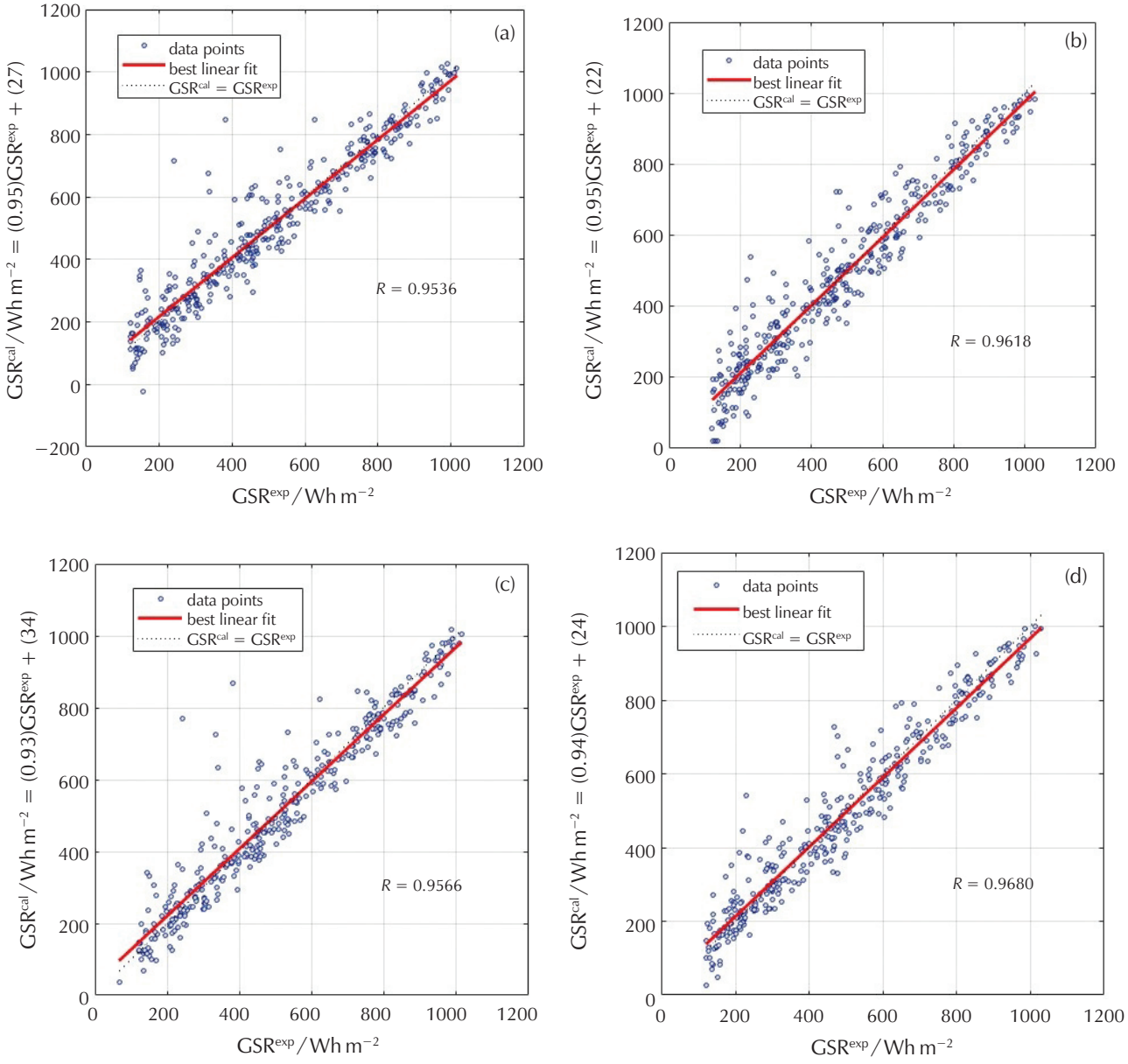

Fig. 5 – Comparison between experimental and predicted global solar radiation: a) SNN validation phase, b) SNN testing phase, c) BANN validation phase, and d) BANN testing phase

where n is the overall number of data points, $y_{i,\mathrm{exp}}$ is the i^{th} expimental value, $y_{i,\mathrm{cal}}$ represents the i^{th} calculated value of the neural network model, and y_e is the mean value of experimental data.

For evaluation purposes, BANN and eleven "good" INNs (neural networks are: 1, 2, 3, 13, 15, 16, 18, 22, 25, 26, and 30) were proposed. Fig. 6 demonstrates that among the 30 INNs, these eleven networks had the most diverse and good performances. INN_{13} gave a lower error value (MPE = 14.5662 %, RMSE = 67.5264 W m^{-2}, and SEP = 13.8227 %) for the total phase, implying the superiority of INN_{13} model which gave the best results on the unseen data.

3.4 Comparison between INN, BANN, and SNN

Table 4 shows the errors of 30 INNs, SNNs, and BANN models of training, validation, test, and total. The outcomes of these networks are inconsistent across all sets. A network with minimal errors in the training dataset may have big errors in the test dataset. The lower RMSE and SEP errors of the INN_{13} for the testing phase were 67.5264 Wh m^{-2} and 13.8227 % respectively. Furthermore, the RMSE and SEP from the BANN model for the testing phase were 62.4856 Wh m^{-2} and 12.7908 %, respectively. The model (BANN) accuracy is significantly improved by combining multiple imperfect models. The two approaches were evaluated according to RMSE, SEP, and

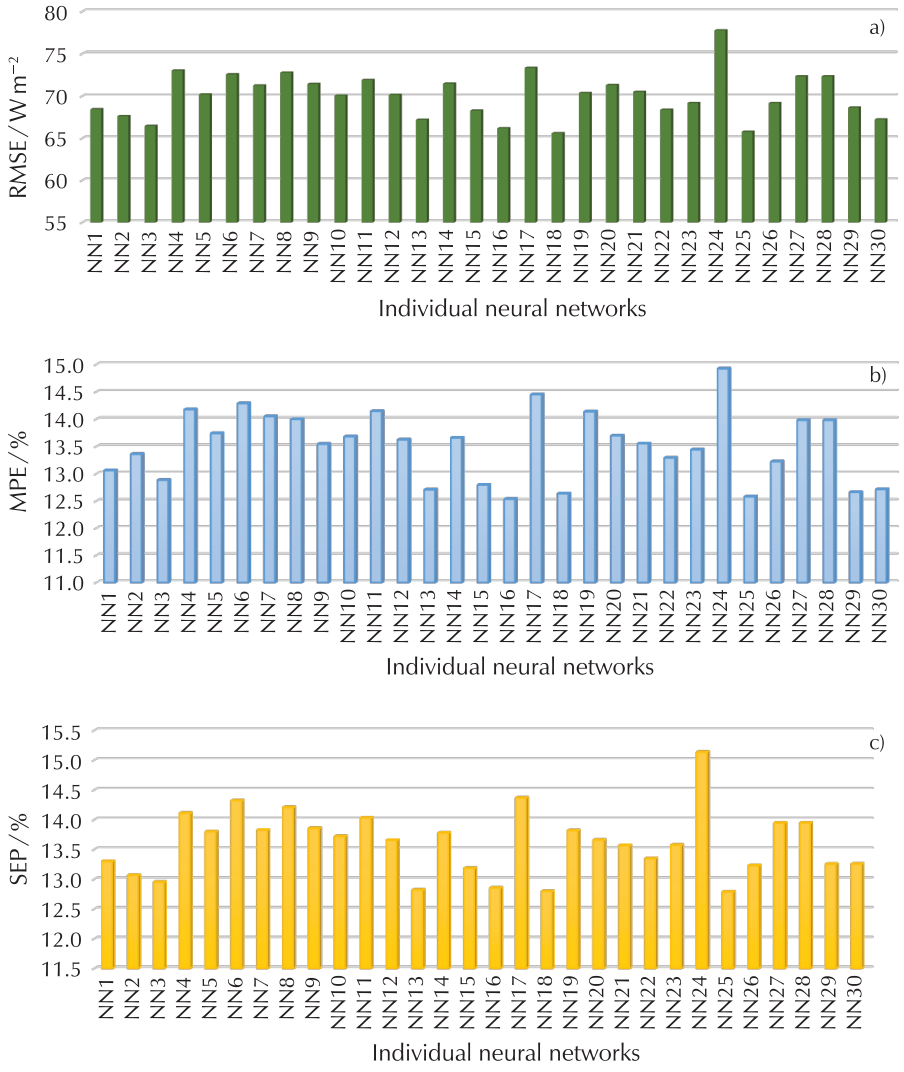

Fig. 6 – Errors obtained for each individual neural network for total database: (a) RMSE, (b) MPE, and (c) SEP

MPE to establish the generated (BANN) model as more credible than the SNN models.

This comparison of the BANN and SNN models is shown in Figs. 7a and 7b. The advantage of the BANN model over the SNN model was demonstrated by a comparison of validation and testing phase results. This demonstrates the robustness of SNN models and the BANN model, which has greater exactness and can be more precise and reliable in the prediction of global solar radiation when unseen data is applied.

Table 4 – Performances of INN, SNN, and BANN models in terms of *R*, MAE, MPE, RMSE, and SPE

		R	MAE / W m^{-2}	MPE / %	RMSE / W m^{-2}	SEP / %
INN_1	Training	0.9610	47.1435	12.5882	67.1635	12.9398
	Validation	0.9525	51.1208	14.4674	76.6738	15.1604
	Testing	0.9600	52.1814	15.4310	69.8713	14.3027
	Total	0.9600	48.0437	13.0597	68.4441	13.2986
INN_2	Training	0.9640	47.5843	12.6655	65.7916	12.5841
	Validation	0.9493	55.2847	16.3270	79.4781	15.7149
	Testing	0.9607	53.5165	15.9460	69.3198	14.1898
	Total	0.9622	48.9456	13.3587	67.6364	13.0651
INN_3	Training	0.9668	45.0790	12.2818	63.6719	12.3069
	Validation	0.9422	52.1937	15.2352	84.6472	16.7369
	Testing	0.9626	51.9116	15.3468	67.8110	13.8809
	Total	0.9638	46.4718	12.8828	66.4765	12.9502
INN_4	Training	0.9572	51.3818	13.7926	72.1796	13.8091
	Validation	0.9479	53.9462	15.4317	80.0534	15.8286
	Testing	0.9577	54.7978	15.9769	72.4171	14.8238
	Total	0.9563	51.9790	14.1744	73.0275	14.1091
INN_5	Training	0.9589	49.1405	13.2518	69.2011	13.5220
	Validation	0.9492	54.0600	15.9739	78.8503	15.5907
	Testing	0.9612	51.8924	15.4010	68.9998	14.1243
	Total	0.9581	49.9066	13.7383	70.2045	13.7968
INN_6	Training	0.9583	50.2839	13.9636	71.3760	14.0178
	Validation	0.9452	57.0546	15.8286	82.114	16.2361
	Testing	0.9579	52.9846	15.3211	71.8980	14.7175
	Total	0.9568	51.2297	14.2854	72.5713	14.3202
INN_7	Training	0.9601	50.6206	13.6161	69.9531	13.4522
	Validation	0.9467	54.5593	15.6510	81.2043	16.0562
	Testing	0.9589	54.7011	15.8990	70.9891	14.5315
	Total	0.9586	51.4215	14.0472	71.2591	13.8248
INN_8	Training	0.9560	50.5514	13.5867	71.5767	13.8712
	Validation	0.9434	55.6797	15.7177	83.4062	16.4916
	Testing	0.9595	54.6889	15.5641	70.8372	14.5004
	Total	0.9550	51.4767	13.9970	72.7722	14.2066
INN_9	Training	0.9586	50.1590	13.2991	70.4095	13.5367
	Validation	0.9492	52.2051	14.1481	79.0788	15.6359
	Testing	0.9579	52.9963	14.8959	71.5429	14.6448
	Total	0.9575	50.6467	13.5433	71.4351	13.8563
INN_{10}	Training	0.9605	47.8047	13.1407	68.1869	13.2630
	Validation	0.9476	53.1083	15.2133	80.8801	15.9921
	Testing	0.9568	55.2127	16.4591	73.2162	14.9874
	Total	0.9587	49.0741	13.6791	70.0673	13.7192
INN_{11}	Training	0.9592	50.8677	13.4755	70.2013	13.5973
	Validation	0.9440	57.5783	16.8159	82.7634	16.3645
	Testing	0.9558	56.9092	16.8197	73.6745	15.0812
	Total	0.9573	52.1412	14.1431	71.9028	14.0309
INN_{12}	Training	0.9607	48.9734	13.0338	68.1828	13.1644
	Validation	0.9447	55.1454	15.9311	82.1242	16.2381
	Testing	0.9565	55.9508	16.0230	72.6823	14.8781
	Total	0.9586	50.2865	13.6216	70.1531	13.6543
INN_{13}	Training	0.9654	46.0540	12.0899	65.4828	12.3316
	Validation	0.9486	56.2848	15.7905	79.3915	15.6978
	Testing	0.9629	50.8105	14.5662	67.5264	13.8227
	Total	0.9635	47.5507	12.7067	67.2039	12.8190

Table 4 – (continued)

		R	MAE / W m^{-2}	MPE / %	RMSE / W m^{-2}	SEP / %
INN_{14}	Training	0.9578	50.4869	13.3521	70.4352	13.4370
	Validation	0.9495	52.2278	14.5857	78.6023	15.5417
	Testing	0.9571	53.1293	15.1674	72.2901	14.7978
	Total	0.9570	50.9246	13.6566	71.4780	13.7779
INN_{15}	Training	0.9628	47.0259	12.2781	66.6456	12.7380
	Validation	0.9502	52.9697	14.6582	78.4081	15.5033
	Testing	0.9595	51.8923	15.0680	70.4067	14.4122
	Total	0.9612	48.1054	12.7944	68.2898	13.1834
INN_{16}	Training	0.9652	44.8391	11.8842	63.8780	12.2965
	Validation	0.9490	51.3384	14.7853	79.4129	15.7020
	Testing	0.9608	51.5260	15.4823	69.8059	14.2893
	Total	0.9630	46.1559	12.5332	66.1954	12.8530
INN_{17}	Training	0.9566	52.3531	14.0740	71.8801	13.9894
	Validation	0.9434	54.9935	15.4795	83.5734	16.5246
	Testing	0.9560	57.0916	16.4221	73.9104	15.1295
	Total	0.9551	53.0900	14.4489	73.3337	14.3655
INN_{18}	Training	0.9690	44.2419	11.7796	61.8780	11.9782
	Validation	0.9432	56.3813	15.8428	84.1506	16.6388
	Testing	0.9566	54.7638	16.2812	73.0082	14.9448
	Total	0.9650	46.5049	12.6349	65.6018	12.7953
INN_{19}	Training	0.9610	49.6754	13.6400	68.4347	13.3602
	Validation	0.9440	56.4846	15.9788	83.2786	16.4663
	Testing	0.9583	54.9811	16.2663	71.4464	14.6251
	Total	0.9589	50.8852	14.1358	70.3582	13.8170
INN_{20}	Training	0.9608	49.6520	13.1038	69.0310	13.0658
	Validation	0.9417	54.5626	15.7424	84.6982	16.7470
	Testing	0.9542	55.8594	16.3940	74.5202	15.2543
	Total	0.9582	50.7622	13.6958	71.3056	13.6574
INN_{21}	Training	0.9612	48.7132	13.0784	68.8432	13.1080
	Validation	0.9456	53.5130	14.8187	82.0312	16.2197
	Testing	0.9582	54.1982	16.0784	71.1230	14.5589
	Total	0.9593	49.7402	13.5518	70.4979	13.5679
INN_{22}	Training	0.9640	47.4297	12.7914	66.6506	12.9129
	Validation	0.9504	51.9073	14.5081	78.0722	15.4369
	Testing	0.9577	54.3245	16.0705	71.6107	14.6587
	Total	0.9620	48.5653	13.2903	68.3802	13.3462
INN_{23}	Training	0.9610	47.7385	12.9521	67.4997	13.1605
	Validation	0.9474	52.5515	14.9656	80.3129	15.8799
	Testing	0.9595	53.1870	15.8274	70.5140	14.4342
	Total	0.9594	48.7633	13.4403	69.1873	13.5729
INN_{24}	Training	0.9502	55.3574	14.7447	77.5343	14.9675
	Validation	0.9430	57.2350	15.7099	83.2881	16.4682
	Testing	0.9554	54.8173	15.5572	73.8441	15.1159
	Total	0.9500	55.4910	14.9222	77.7701	15.1349
INN_{25}	Training	0.9653	44.9974	12.1271	64.3141	12.3995
	Validation	0.9561	48.8730	13.5462	73.5154	14.5359
	Testing	0.9610	52.3215	15.2251	69.0457	14.1337
	Total	0.9640	46.1158	12.5782	65.7720	12.7867
INN_{26}	Training	0.9629	47.2317	12.5265	67.0250	12.6602
	Validation	0.9443	54.5213	15.7815	82.9192	16.3953
	Testing	0.9585	53.2841	16.2463	71.0661	14.5472
	Total	0.9606	48.5640	13.2230	69.1814	13.2286

Table 4 – (continued)

		R	MAE / W m^{-2}	MPE / %	RMSE / W m^{-2}	SEP / %
INN_{27}	Training	0.9633	45.7982	12.1920	65.1769	12.6293
	Validation	0.9566	52.2369	13.7019	71.7125	13.6813
	Testing	0.9578	54.5804	15.5618	71.5605	14.6484
	Total	0.9561	52.4105	13.9793	72.3418	13.9450
INN_{28}	Training	0.9566	52.2369	13.7019	71.7125	13.6813
	Validation	0.9506	51.6319	14.6198	77.9242	15.4076
	Testing	0.9578	54.5804	15.5618	71.5605	14.6484
	Total	0.9561	52.4105	13.9793	72.3418	13.9450
INN_{29}	Training	0.9613	46.8625	12.0862	66.7803	12.7641
	Validation	0.9455	55.7374	15.2728	81.8007	16.1741
	Testing	0.9612	52.6002	14.6511	68.9905	14.1224
	Total	0.9596	48.3217	12.6605	68.6472	13.2527
INN_{30}	Training	0.9642	45.7545	12.1616	65.0989	12.7690
	Validation	0.9481	51.8555	14.6248	79.7014	15.7590
	Testing	0.9591	53.3470	15.2213	70.4295	14.4169
	Total	0.9620	47.1219	12.7132	67.2396	13.2547
SNN	Training	0.9624	47.8535	12.8494	67.2010	12.9266
	Validation	0.9541	50.6691	14.7987	75.3743	14.9034
	Testing	0.9618	51.3457	15.4556	68.3968	14.0008
	Total	0.9615	48.4834	13.3044	68.1802	13.2305
$BANN_{(stacking\ 30\ net)}$	Validation	0.9566	46.0080	12.6926	72.8758	14.4094
	Testing	0.9680	46.3138	12.9661	62.4856	12.7908

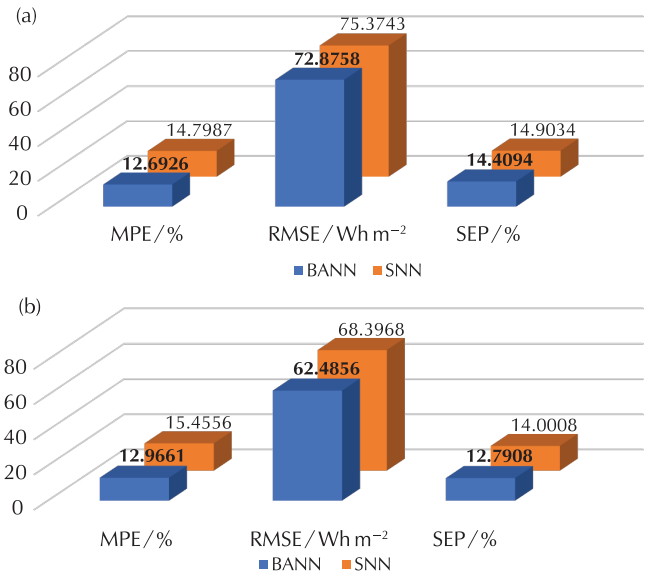

Fig. 7 – MPE, RMSE, and SEP of BANN and SNN: (a) validation phase, and (b) test phase

3.5 Comparison with other models

In order to evaluate the importance of the obtained results, they were compared with similar studies developed by other researchers, especially with the models that had the same inputs as we used. It was found that, in all models, the goal was to predict solar radiation. These results confirm the strength and accuracy of BANN model for global solar radiation. The results obtained from these mentioned models, and results in this work are presented in Table 5.

Table 5 – Overview of various models for predicting global solar radiation

Refs.	Location	Models	Evaluation Index
This study	Bouzareah (Algeria)	BANN	$R = 0.9680$
Guermoui et al.[46]	Ghardaïa (Algeria)	Support vector machine "SVM"	$R = 93.06$
Linares-Rodríguez et al.[47]	Spain	Multilayered perception "ANN-MLP"	$R = 0.9400$
Fadare[48]	Nigeria	Multilayered perception, feedforward, back-propagation "MLP-FBP"	$R = 0.9560$
Mohammadi et al.[49]	Isfahan (Iran)	Adaptive neuro-fuzzy inference system (ANFIS)	$R = 0.9932$
Mehdi Lotfinejad et al.[50]	Jask (Iran)	Bat neural network (BNN)	$R = 0.9810$

4 Conclusion

The current study aimed to predict the value of hourly global solar radiation in Bouzareah using BANN. A comparison of BANN and SNN models found that the BANN model performed the best: The validation phase had a root mean squared error of 72.8758 Wh m^{-2} for BANN and 75.3748 Wh m^{-2} for SNN, whereas the testing phase had a root mean squared error of 62.4856 Wh m^{-2} for BANN, and 68.3968 Wh m^{-2} for SNN. The BANN model had greater precision and could describe the prediction of hourly global solar radiation more accurately compared to the SNN model. This confirms that such BANN model can give a more accurate and robust prediction than SNN model. The robust predictions of BANN model was proven by this comparison when applied to unseen databases.

The BANN model can be utilised to predict solar radiation for locations that have no measurement equipment (solarimeters/pyranometers) and relevant systems, when the actual data set available is small, in case of a group of outliers that must be excluded, or missing data, as well as to install solar-energy systems, and assess the thermal conditions in building studies in Algeria.

ACKNOWLEDGEMENTS

The authors gratefully acknowledge the help of Ministry of Higher Education of Algeria (PRFU Projects N°A16N01UN260120220004) and the group of Laboratory of Biomaterials and Transport Phenomena in the University of Medea and the University of Relizane throughout this project.

References
Literatura

1. *E. W. McFarland*, Solar energy setting the economic bar from the top-down, Energy Environ. Sci. **7** (2014) 846–854, doi: https://doi.org/10.1039/C3EE43714K.
2. *J. L. Chen, B. B. Xiao, C. D. Chen, Z. F. Wen, Y. Lv. Jiang, M. Q. Wu, G. S. Li*, Estimation of monthly-mean global solar radiation using MODIS atmospheric product over China, J. Atmos. Solar-Terrestrial Phys. **110** (2014) 63–80, doi: https://doi.org/10.1016/j.jastp.2014.01.017.
3. *S. Bamehr, S. Sabetghadam*, Estimation of global solar radiation data based on satellite-derived atmospheric parameters over the urban area of Mashhad, Iran, Environ. Sci. Pollut. Res. **28** (6) (2021) 7167–7179, doi: https://doi.org/10.1007/s11356-020-11003-8.
4. *Z. Jiandong, T. Hanzhong, C. Susu*, Numerical simulation for structural parameters of flat-plate solar collector. Sol. Energy **117** (2015) 192–202, doi: https://doi.org/10.1016/j.solener.2015.04.027.
5. *İ. Uçkan, K. M. Khudhur*, Improving of global solar radiation forecast by comparing other meteorological parameter models with sunshine duration models, Environ. Sci. Pollut. Res. **29** (25) (2022) 37867–37881, doi: https://doi.org/10.1007/s11356-022-18781-3.
6. *D. L. Hunt, R. B. Haynes, S. E. Hanna, K. Smith*, Effects of computer-based clinical decision support systems on physician performance and patient outcomes: a systematic review, JAMA **280** (15) (1998) 1339–1346, doi: https://doi:10.1001/jama.280.15.1339.
7. *R. Marquez, C. F. Coimbra*, Forecasting of global and direct solar irradiance using stochastic learning methods, ground experiments and the NWS database, Sol. Energy **85** (5) (2011) 746–756, doi: https://doi.org/10.1016/j.solener.2011.01.007.
8. *F. Antonanzas-Torres, R. Urraca, J. Antonanzas, J. Fernandez-Ceniceros, F. J. Martinez-de-Pison*, Generation of daily global solar irradiation with support vector machines for regression, Energy Convers. Manag. **96** (2015) 277–286, doi: https://doi.org/10.1016/j.enconman.2015.02.086.
9. *P. A. Rocha, V. O. Santos*, Global horizontal and direct normal solar irradiance modeling by the machine learning methods XGBoost and deep neural networks with CNN-LSTM layers: a case study using the GOES-16 satellite imagery, Int. J. Energy Environ. Eng. **13** (2022) 1271–1286, doi: https://doi.org/10.1007/s40095-022-00493-6.
10. *M. H. Al-Shamisi, A. H. Assi, H. A. Hejase*, Artificial neural networks for predicting global solar radiation in Al Ain city-UAE, Int. J. Green Energy **10** (5) (2013) 443–456, doi: https://doi.org/10.1080/15435075.2011.641187.
11. *S. S. Priya, M. H. Iqbal*, Solar radiation prediction using artificial neural network, Int. J. Comput. Appl. **116**(16) (2015) 772–781, doi: https://doi.org/10.1016/j.rser.2013.08.055.
12. *Ö. Çelik, A. Teke, H. B. Yıldırım*, The optimized artificial neural network model with Levenberg–Marquardt algorithm for global solar radiation estimation in Eastern Mediterranean Region of Turkey, J. Clean. Prod. **116** (2016) 1–12, doi: https://doi.org/10.1016/j.jclepro.2015.12.082.
13. *K. Chiteka, C. C. Enweremadu*, Prediction of global horizontal solar irradiance in Zimbabwe using artificial neural networks. J. Clean. Prod. **135** (2016) 701–711, doi: https://doi.org/10.1016/j.jclepro.2016.06.128.
14. *E. F. Alsina, M. Bortolini, M. Gamberi, A. Regattieri*, Artificial neural network optimisation for monthly average daily global solar radiation prediction, Energy Convers. Manag. **120** (2016) 320–329, doi: https://doi.org/10.1016/j.enconman.2016.04.101.
15. *C. M. Siham, H. Salah, L. Maamar, K. Latifa*, Artificial neural networks based prediction of hourly horizontal solar radiation data: case study, Int. J. Appl. Decis. Sci. **10** (2) (2017) 156–174, doi: https://doi.org/10.1504/ijads.2017.10004222.
16. *X. Xue*, Prediction of daily diffuse solar radiation using artificial neural networks, Int. J. Hydrog. Energy **42** (47) (2017) 28214–2822, doi: https://doi.org/10.1016/j.ijhydene.2017.09.150.
17. *M. Premalatha, C. Naveen*, Analysis of different combinations of meteorological parameters in predicting the horizontal global solar radiation with ANN approach: A case study, Renew. Sustain. Energy Rev. **91** (2018) 248–258, doi: https://doi.org/10.1016/j.rser.2018.03.096.
18. *P. A. Rocha, J. L. Fernandes, A. B. Modolo, R. J. Lima, M. E. da Silva, C. A. Bezerra*, Estimation of daily, weekly and monthly global solar radiation using ANNs and a long data set: a case study of Fortaleza, in Brazilian Northeast region, Int. J. Energy Environ. Eng. **10**(3) (2019) 319–334, doi: https://doi.org/10.1007/s40095-019-0313-0.
19. *M. Marzouq, Z. Bounoua, H. El Fadili, A. Mechaqrane, K. Zenkouar, Z. Lakhliai*, New daily global solar irradiation estimation model based on automatic selection of input parameters using evolutionary artificial neural networks, J. Clean. Prod. **209** (2019) 1105–1118, doi: https://doi.org/10.1016/j.jclepro.2018.10.254.
20. *C. G. Ozoegwu*, Artificial neural network forecast of monthly mean daily global solar radiation of selected locations based on time series and month number, J. Clean. Prod. **216** (2019)

1–13, doi: https://doi.org/10.1016/j.jclepro.2019.01.096.

21. *D. Guijo-Rubio, A. M. Durán-Rosal, P. A. Gutiérrez, A. M. Gómez-Orellana, C. Casanova-Mateo, J. Sanz-Justo, C. Hervás-Martínez*, Evolutionary artificial neural networks for accurate solar radiation prediction, Energy **210** (2020) 118374, doi: https://doi.org/10.1016/j.energy.2020.118374.
22. *O. M. Babatunde, J. L. Munda, Y. Hamam*, Exploring the potentials of artificial neural network trained with differential evolution for estimating global solar radiation, Energies **13** (10) (2020) 2488, doi: https://doi.org/10.3390/en13102488.
23. *B. Amiri, R. Dizène, K. Dahmani*, Most relevant input parameters selection for 10-min global solar irradiation estimation on arbitrary inclined plane using neural networks, Int. J. Sustain. Energy **39** (8) (2020) 779–803, doi: https://doi.org/10.1080/14786451.2020.1758104.
24. *D. Shah, K. Patel, M. Shah*, Prediction and estimation of solar radiation using artificial neural network (ANN) and fuzzy system: a comprehensive review, Int. J. Energy Water Res. **5** (2) (2021) 219–233, doi: https://doi.org/10.1007/s42108-021-00113-9.
25. *E. S. Elmolla, M. Chaudhuri, M. M. Eltoukhy*, The use of artificial neural network (ANN) for modeling of COD removal from antibiotic aqueous solution by the Fenton process. J. Hazard. Mater. **179** (1-3) (2010) 127–134, doi: https://doi.org/10.1016/j.jhazmat.2010. 02.068.
26. *J. Zhang*, Inferential estimation of polymer quality using bootstrap aggregated neural networks, Neural Networks **12** (1999) 927–938, doi: https://doi.org/10.1016/S0893-6080(99)00037-4.
27. *L. K. Hansen, P. Salamon*, Neural network ensembles, IEEE Trans. Pattern Anal. Mach. Intell. **12** (10) (1990) 993–1001, doi: https://doi.org/10.1109/34.58871.
28. *D. V. Sridhar, R. C. Seagrave, E. B. Bartlett*, Process modeling using stacked neural networks, AIChE Journal **42** (9) (1996) 2529–2539, doi: https://doi.org/10.1002/aic.690420913.
29. *J. Zhang, E. B. Martin, A. J. Morris, C. Kiparissides*, Inferential estimation of polymer quality using stacked neural networks, Comp. Chem. Eng. **21** (1997) S1025–S1030, doi: https://doi.org/10.1016/S0098-1354(97)87637-5.
30. *D. H. Wolpert*, Stacked generalization, Neural networks **5** (2) (1992) 241–259, doi: https://doi.org/10.1016/S0893-6080(05)80023-1.
31. *M. A Jallal, S. Chabaa, A. Zeroual*, A new artificial multi-neural approach to estimate the hourly global solar radiation in a semi-arid climate site, Theor. Appl. Climatol. **139** (3) (2020) 1261–1276, doi: https://doi.org/10.1007/s00704-019-03033-1.
32. *L. Benali, G. Notton, A. Fouilloy, C. Voyant, R. Dizene*, Solar radiation forecasting using artificial neural network and random forest methods: Application to normal beam, horizontal diffuse and global components, Renew. Energy **132** (2019) 871–884, doi: https://doi.org/10.1016/j.renene.2018.08.044.
33. *H. C. Cheng, K. Yu, C. Hsu, M. Chan, C. L. Tseng*, Estimating Solar Irradiance on Tilted Surface with Arbitrary Orientations and Tilt Angles. Energies **12** (8) (2019) 1427, doi: https://doi.org/10.3390/en12081427.
34. *N. Premalatha, A. V. Arasu*, Prediction of solar radiation for solar systems by using ANN models with different back propagation algorithms, J. Appl. Res. Technol. **14** (3) (2016) 206–214, doi: https://doi.org/10.1016/j.jart.2016.05.001.
35. *H. K. Elminir, F. F. Areed, T. S. Elsayed*, Estimation of solar radiation components incident on Helwan site using neural networks, Sol. Energy **79** (3) (2005) 270–279, doi: https://doi.org/10.1016/j.solener.2004.11.006.
36. *S. P. Durrani, S. Balluf, L, Wurzer, S. Krauter*, Photovoltaic yield prediction using an irradiance forecast model based on multiple neural networks, J. Mod. Power Syst. Clean Energy **6** (2) (2018) 255–267, doi: https://doi.org/10.1007/s40565-018-0393-5.
37. *A. Rezrazi, S. Hanini, M. Laidi*, An optimisation methodology of artificial neural network models for predicting solar radiation: a case study, Theor. Appl. Climatol. **123** (3) (2016) 769–783, doi: https://doi.org/10.1007/s00704-015-1398-x.
38. *K. Dahmani, R. Dizene, G. Notton, C. Paoli, C. Voyant, M. L. Nivet*, Estimation of 5-min time-step data of tilted solar global irradiation using ANN (Artificial Neural Network) model, Energy **70** (2014) 374–381, doi: https://doi.org/10.1016/j.energy.2014.04.011.
39. *S. Kalogirou, E. Mathioulakis, V. Belessiotis*, Artificial Neural Networks for the Performance Prediction of Large Solar Systems, Renew. Energy **63** (2014) 90–97, doi: https://doi:10.1016/j.renene.2013.08.049.
40. *Y. Ammi, L. Khaouane, S. Hanini*, Stacked neural networks for predicting the membranes performance by treating the pharmaceutical active compounds, Neural Comput. Appl. **33** (19) (2021) 12429–12444, doi: https://doi.org/10.1007/s00521-021-05876-0.
41. *G. Liu, L. Jia, B. Kong, K. Guan, H. Zhang*, Artificial neural network application to study quantitative relationship between silicide and fracture toughness of Nb-Si alloys. Mater. Des. **129** (2017) 210–218, doi: https://doi.org/10.1016/j.matdes.2017.05.027.
42. *L. Khaouane, Y. Ammi, S. Hanini*, Modeling the retention of organic compounds by nanofiltration and reverse osmosis membranes using bootstrap aggregated neural networks, Arab. J. Sci. Eng. **42** (4) (2017) 1443–1453, doi: https://doi.org/10.1007/s13369- 016-2320-2.
43. *B. Efron, R. Tibshirani*, An Introduction to Bootstrap. Chapman and Hall, London, 1993.
44. *Y. Ammi, L. Khaouane, S. Hanini*, A model based on bootstrapped neural networks for modeling the removal of organic compounds by nanofiltration and reverse osmosis membranes. Arab. J. Sci. Eng. **43** (11) (2018) 6271–6284, doi: https://doi.org/10.1007/s13369-018-3484-8.
45. *J. Kiseľák, Y. Lu, J.* Švihra*, P. Szépe, M. S. Stehlík*, "SPOCU": scaled polynomial constant unit activation function. Neural Comput. Appl. **33** (8) (2021) 3385–3401, doi: https://doi.org/10.1007/s00521-020-05182-1.
46. *M. Guermoui, K. Bouchouicha, S. Benkaciali, K. Gairaa, N. Bailek*, New soft computing model for multi-hours forecasting of global solar radiation. Eur. Phys. J. Plus **137** (1) (2022) 162, doi: https://doi.org/10.1140/epjp/s13360-021-02263-5.
47. *A. Linares-Rodriguez, J. A. Ruiz-Arias, D. Pozo-Vazquez, J. Tovar-Pescador*, An artificial neural network ensemble model for estimating global solar radiation from Meteosat satellite images. Energy **61** (2013) 636–645, doi: https://doi.org/10.1016/j.energy.2013.09.008
48. *D. A. Fadare*, Modelling of solar energy potential in Nigeria using an artificial neural network model. Appl. Energy **86** (9) (2009) 1410–1422, doi: https://doi:10.1016/j.apenergy.2008.12.005.
49. *K. Mohammadi, S. Shamshirband, A. Kamsin, P. C. Lai, Z. Mansor*, Identifying the most significant input parameters for predicting global solar radiation using an ANFIS selection procedure. Renew. Sustain. Energy Rev. **63** (2016) 423–434, doi: https://doi.org/10.1016/j.rser.2016.05.065.
50. *M. M. Lotfinejad, R. Hafezi, M. Khanali, S. S. Hosseini, M. Mehrpooya*, S. Shamshirband, A comparative assessment of predicting daily solar radiation using bat neural network (BNN), generalized regression neural network (GRNN), and neuro-fuzzy (NF) system: A case study. Energies **11** (5) (2018) 1188, doi: https://doi.org/10.3390/en11051188.

SAŽETAK

Predviđanje globalnog Sunčeva zračenja po satu: usporedba neuronske mreže / *bootstrap* agregacija

Abdennasser Dahmani,[a,b*] *Yamina Ammi*,[b] *Salah Hanini*,[b] *Mohamed Redha Yaiche*[c] i *Hamid Zentou*[d]

U ovom radu istražena je primjena pojedinačnih i *bootstrap* agregiranih neuronskih mreža u predviđanju globalnog Sunčeva zračenja po satu. Baza od 3606 podatkovnih točaka dobivena je iz Centra za razvoj obnovljivih izvora energije, radiometrijske postaje 'Shems' u Bouzareahu. Pojedinačne neuronske mreže i *bootstrap* agregirane neuronske mreže izgrađene su zajedno. Preciznost i trajnost modela neuronskih mreža generiranih uz nepotpuni set podataka za treniranje poboljšani su primjenom *bootstrap* agregiranih neuronskih mreža. Da bi se proizveli brojni setovi podataka za treniranje, primijenjeno je ponovljeno uzorkovanje podataka primjenom metodologije slučajnog uzorkovanja sa zamjenom. Za svaku podatkovnu točku izgrađena je neuronska mreža. Pojedinačne neuronske mreže su potom kombinirane u *bootstrap* agregirane neuronske mreže. Uspoređene su eksperimentalne i predviđene vrijednosti globalnog Sunčeva zračenja te su tijekom faza testiranja dobivene niže vrijednosti srednje kvadratne pogreške za pojedinačne odnosno *bootstrap* agregirane neuronske mreže (68,3968 i 62,4856 Wh m^{-2}). Rezultati su pokazali da je model *bootstrap* agregiranih neuronskih mreža precizniji i robusniji od pojedinačnih neuronskih mreža.

Ključne riječi
Predviđanje, globalno Sunčevo zračenje po satu, neuronske mreže, bootstrap agregacija

[a] *Department of Mechanical Engineering, Faculty of Science and Technology, GIDD Industrial Engineering and Sustainable Development Laboratory, University of Relizane, Bourmadia, 48 000, Relizane, Alžir*
[b] *Laboratory of Biomaterials and Transport Phenomena (LBMPT), University of Medea, urban pole, 26 000, Medea, Alžir*
[c] *Renewable Energy Development Center (CDER), Postal Box 62, Observatory Road Bouzareah 16 340, Algiers, Alžir*
[d] *Department of Chemical and Environmental Engineering, University Putra Malaysia, 43 400 Serdang, Malezija*

Izvorni znanstveni rad
Prispjelo 9. listopada 2022.
Prihvaćeno 24. siječnja 2023.